河南师范大学
HENAN NORMAL UNIVERSITY

外泌体与脂代谢

报告人：卢荣华

Xin xiang China
AUG, 2016

汇 报 提 纲

- 外泌体研究概况
- 外泌体功能
- 外泌体与脂肪代谢

河南师范大学
HENAN NORMAL UNIVERSITY

外泌体研究概况

概念：外泌体exosome：是细胞主动向胞外分泌的大小均一的囊泡样小体，具有抗肿瘤免疫、促血管新生等生理功能。不同类型的细胞可以释放出外泌体，正常生理状态下血液、尿液、乳汁和支气管灌洗液中也能分离到外泌体,直径在40~100 nm

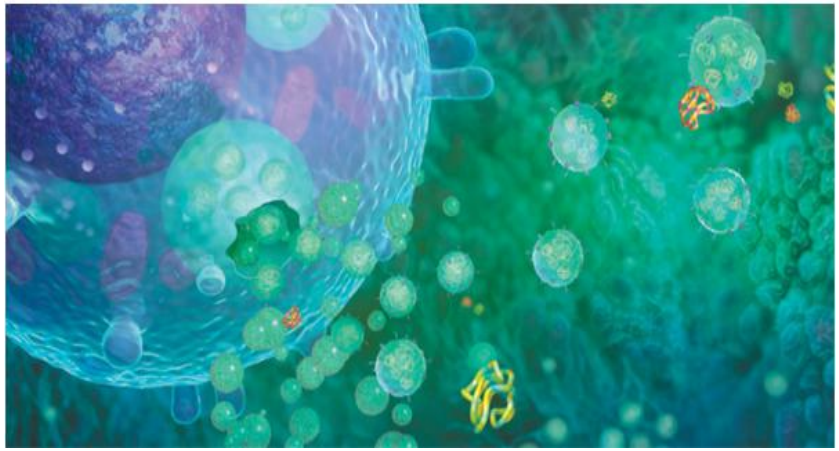

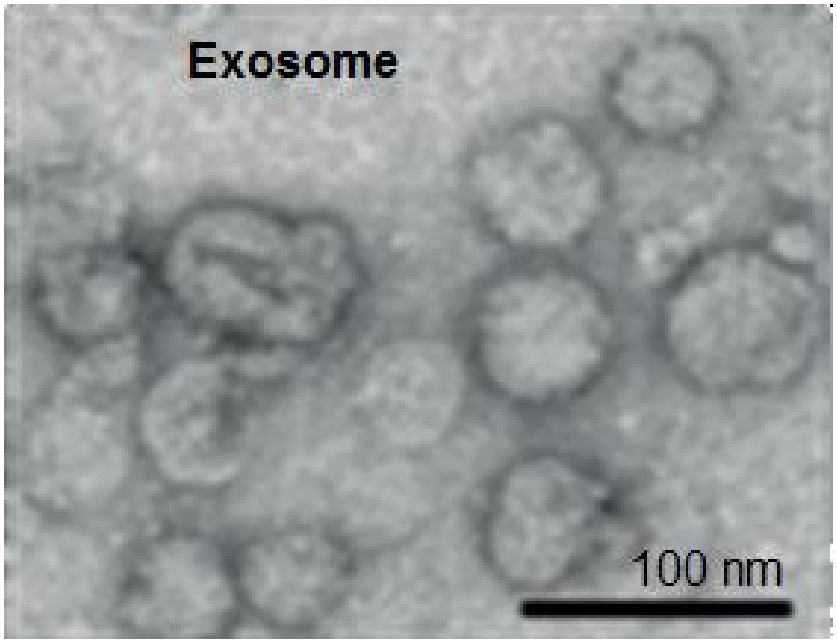

外泌体研究概况

Exosome来源于晚期核内体(也称为多囊泡体)的囊泡，外泌体是目前为止定义最明确的囊泡。细胞内内溶酶体微粒(endolysosomal vesicle)内陷形成多囊泡体(multi-vesicular body)，在刺激作用下，多囊泡体与细胞膜融合，向胞外分泌的大小均一，直径在40~100 nm 的囊泡为外泌体。

2013年诺贝尔奖揭晓，美国、德国3位科学家James E. Rothman, Randy W. Schekman和Thomas C. Südhof因 "发现细胞内的主要运输系统--囊泡运输的调节机制"，荣获2013年诺贝尔生理学或医学奖。这一奖项的授予，无疑将囊泡的研究推向了新的高潮。

外泌体研究概况

尽管外泌体最初在1987年就被发现，但人们一直认为它只是一种细胞的废弃物。然而最近几年，人们发现这种微小膜泡中含有细胞特异的蛋白、脂质和核酸，能作为信号分子传递给其他细胞从而改变其他细胞的功能。这些发现点燃了人们对细胞分泌膜泡的兴趣。

最近的研究发现外泌体在很多生理病理上起着重要的作用，如免疫中抗原呈递、肿瘤的生长与迁移、组织损伤的修复等。不同细胞分泌的外泌体具有不用的组成成分和功能，可作为疾病诊断的生物标志物。

外泌体研究概况

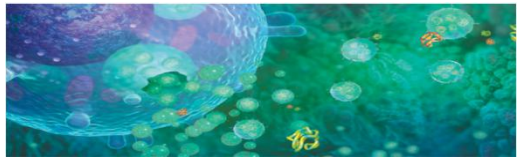

结构与内容物： 外泌体的分泌最早是由Johnstone 等在1987年研究网织红细胞的成熟过程中发现的。

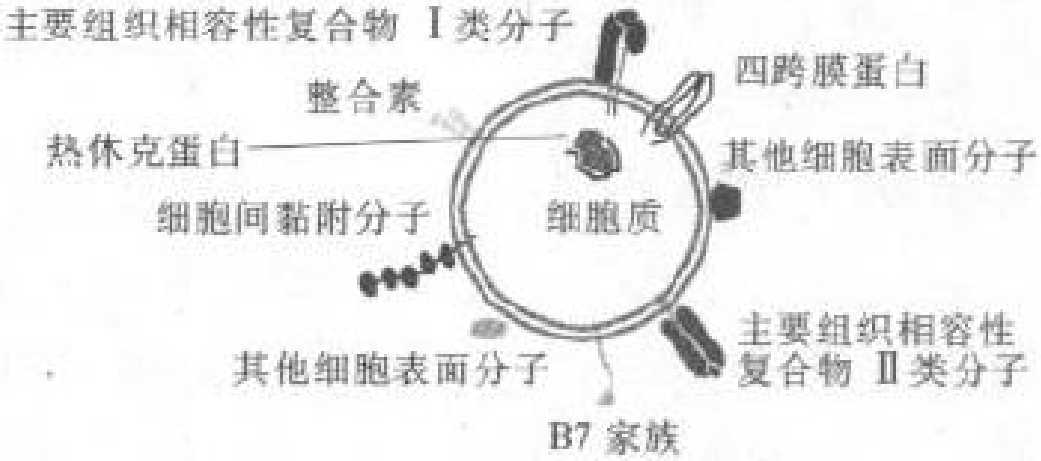

外泌体为脂质双层膜包裹的纳米级囊泡，内含细胞质。其80%的蛋白质成分在不同细胞来源的外泌体中是保守的，包括主要组织相容性复合物分子，热休克蛋白，四跨膜蛋白等

图 1 外泌体结构示意图

外泌体研究概况

结构与内容物：由于其特殊的形成方式，外泌体不含有内质网内的蛋白质，而高表达细胞内源性蛋白质如Alix、Tsg101。肠上皮细胞来源的外泌体含有多种代谢酶及肠组织特异性A33抗原，B细胞来源的外泌体富含CD86和MHC分子，T细胞来源的外泌体表面有促凋亡的FasL受体。外泌体内的RNA主要为小RNA，包括miRNA。miRNA不仅仅是遗传信息的内源性调控者，也是调节细胞通讯的分泌因子及疾病的生物。

外泌体研究概况

外泌体对靶细胞的调节作用： 外泌体靶向细胞的方式主要有三种：一是直接与靶细胞的胞膜融合，同时释放mRNA、miRNA进入细胞质；二是通过内吞作用被靶细胞摄取；三是识别细胞表面的特异性受体(图**1**)。

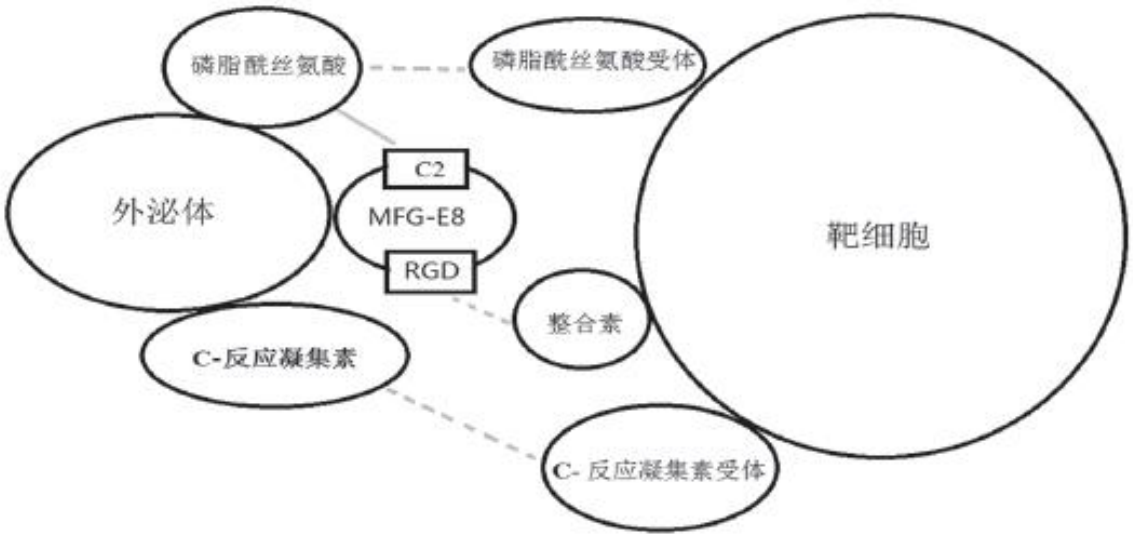

图1 外泌体与靶细胞表面特异性受体

外泌体研究概况

外泌体其他的调节作用：外泌体表面有多种生长因子、细胞因子(如VEGF、SCF)，并且几乎所有的外泌体内都含有生理活性的脂质成分如1-磷酸鞘氨醇(sphingosine-1-phosphate, S1P)、神经酰胺-1-磷酸(ceramide-1-phosphate, C1P)。外泌体进入靶细胞后，这些旁分泌因子直接与细胞相互作用，如S1P、C1P可抑制细胞凋亡和刺激血管新生。此外，外泌体还可水平转移miRNA至受体细胞，miRNA作为信号分子直接传达遗传信息，调节细胞功能。

外泌体研究概况

获取外泌体的方法：具体来说，exosome的研究方式是分离/捕获小囊泡，并分析它所携带的因子。就目前而言，人们多采用超速离心、磁珠免疫捕获、沉淀或过滤的方法，对exosome进行前期的分离。之后利用电镜来分析其大小和形态，利用流式细胞仪来分析细胞表面标记，通过Western blot和ELISA等方法对蛋白进行分析，或通过qPCR和新一代测序（NGS）来分析RNA。

外泌体研究概况

离心法

这是目前外泌体提取最常用的方法。简单来说，收集细胞培养液以后依次在300 g、2 000 g、10 000 g离心去除细胞碎片和大分子蛋白质，最后100 000 g离心得到外泌体[Sheldon H,et al.2010]。此种方法得到的外泌体量多，但是纯度不足，电镜鉴定时发现外泌体聚集成块，由于微泡和外泌体没有非常统一的鉴定标准，也有一些研究认为此种方法得到的是微泡不是外泌体。

外泌体研究概况

过滤离心

过滤离心是利用不同截留相对分子质量(MWCO)的超滤膜离心分离外泌体。截留相对分子质量是指能自由通过某种有孔材料的分子中最大分子的相对分子质量。外泌体是一个囊状小体，相对分子质量大于一般蛋白质，因此选择不同大小的MWCO膜可使外泌体与其他大分子物质分离[Lai RC, et al.,2010]。

外泌体研究概况

密度梯度离心

实验中常用蔗糖密度梯度离心法,预先将两种浓度蔗糖溶液(如2.5 M 和0.25 M)配成连续梯度体系置于超速离心管中，样本铺在蔗糖溶液上，100 000 g离心16 h，外泌体会沉降到等密度区(1.10~1.18 g/ml)。用此种方法分离到的外泌体纯度高，但是前期准备工作繁杂，耗时，量少。

外泌体研究概况

免疫磁珠法

预先使磁珠包被针对外泌体相关抗原的抗体(如CD9、CD63、Alix)与外泌体共同孵育，蒸馏水冲洗后，重悬于PBS缓冲液中[Jansen et al,2009]。

色谱法

样品中大分子不能进入凝胶孔，只能沿多孔凝胶粒子之间的空隙通过色谱柱，首先被流动相洗脱出来；小分子可进入凝胶中绝大部分孔洞，在柱中受到更强地滞留，更慢地被洗脱出[Chen et al,2011]。分离到的外泌体在电镜下大小均一，但需特殊的设备，

外泌体研究概况-外泌体功能

母乳exosome small RNA测序发现免疫相关miRNA

研究者通过small RNA测序对母乳exosome miRNA进行了研究，发现大部分miRNA与免疫系统相关，猜测母乳中的miRNA对婴儿免疫系统的形成起到不可或缺的作用，为研究母乳的生理作用提供新的研究方向（Kogure T, et al. Hepatology. 2011）

HSP70+人结肠癌细胞来源的外泌体在体外可刺激NK细胞直接杀伤肿瘤细胞，携带肿瘤抗原的外泌体可将其表面的MHC抗原肽复合物传递给树突状细胞，增强抗肿瘤免疫。

外泌体研究概况---外泌体功能

Exosome miRNA研究揭示肝癌细胞通讯新机制

研究者通过对肝癌细胞及其分泌的exosome中miRNA进行qPCR检测，通过生物信息学分析，主要在exosome中表达的11个miRNA可能靶向TAK1、TAB2基因。将提取的exosome加入受体细胞Hep3B后，检测到受体细胞TAK1/TAB2/Jnk/p38蛋白显著下调，为肿瘤细胞的生存制造合适的生长环境。该研究揭示了exosome介导miRNA的转移在肝癌细胞通讯中是一个非常重要的机制。（Vlassov AV, et al. Bba-Gen Subjects. 2012）

外泌体研究概况-外泌体功能

揭示exosome介导的细胞间抗病毒作用

研究者分别对肝窦状内皮细胞(LSECs)及α干扰素(IFN-α)处理的LSECs细胞培养上清的exosome进行了miRNA及mRNA芯片检测，筛选出了表达差异显著的618个mRNA和3个miRNA。随机挑选了11个mRNA和3个miRNA进行后续qPCR验证，证实了这些mRNA及miRNA在IFN-α处理的LSECs细胞培养上清exosome中表达量上调。

外泌体研究概况—外泌体功能

研究者将exosome中发现的这11个mRNA的表达载体和3个miRNA的模拟物mimics（RiboBio Co. Ltd.）分别转染到共表达HBV（乙型肝炎病毒）的HepG2细胞，结果发现HBV的DNA及RNA表达量都有所降低，从而揭示了exosome介导细胞间抗病毒作用的传递是一个非常重要的机制。 (Li J, et al. Nat Immunol. 2013)

外泌体与脂肪及肝脏组织互作

Adipocyte exosomes induce transforming growth factor beta pathway dysregulation in hepatocytes: a novel paradigm for obesity-related liver disease

Emily S. Koeck, MD,[a] Tatiana Iordanskaia, PhD,[a] Samantha Sevilla, MFS,[a] Sarah C. Ferrante, BS,[b,c] Monica J. Hubal, PhD,[a,b,c] Robert J. Freishtat, MD,[b,c,d] and Evan P. Nadler, MD[a,b,]*

[a] *Sheikh Zayed Institute for Pediatric Surgical Innovation, Children's National Medical Center, Washington, DC*
[b] *Department of Integrative Systems Biology, George Washington University School of Medicine and Health Sciences, Washington, DC*
[c] *Research Center for Genetic Medicine, Children's National Medical Center, Washington, DC*
[d] *Division of Emergency Medicine, Children's National Medical Center, Washington, DC*

脂肪细胞外泌体诱导转化生长因子β1蛋白(TGFβ1）路径失调: 一种与肥胖相关疾病的新范式

河南师范大学 HENAN NORMAL UNIVERSITY

摘要

ABSTRACT

Background: The pathogenesis of nonalcoholic fatty liver disease (NAFLD) has been attributed to increased systemic inflammation and insulin resistance mediated by visceral adipose tissue (VAT), although the exact mechanisms are undefined. Exosomes are membrane-derived vesicles containing messenger RNA, microRNA, and proteins, which have been implicated in cancer, neurodegenerative, and autoimmune diseases, which we postulated may be involved in obesity-related diseases. We isolated exosomes from VAT, characterized their content, and identified their potential targets. Targets included the transforming growth factor beta (TGF-β) pathway, which has been linked to NAFLD. We hypothesized that adipocyte exosomes would integrate into HepG2 and hepatic stellate cell lines and cause dysregulation of the TGF-β pathway.

Methods: Exosomes from VAT from obese and lean patients were isolated and fluorescently labeled, then applied to cultured hepatic cell lines. After incubation, culture slides were imaged to detect exosome uptake. In separate experiments, exosomes were applied to cultured cells and incubated 48-h. Gene expression of TGF-β pathway mediators was analyzed by polymerase chain reaction, and compared with cells, which were not exposed to exosomes.

Results: Fluorescent-labeled exosomes integrated into both cell types and deposited in a perinuclear distribution. Exosome exposure caused increased tissue inhibitor of matrix metalloproteinase-1 (TIMP-1) and integrin αvβ-5 expression and decreased matrix metalloproteinase-7 and plasminogen activator inhibitor-1 expression in to HepG2 cells and increased expression of TIMP-1, TIMP-4, Smad-3, integrins αvβ-5 and αvβ-8, and matrix metalloproteinase-9 in hepatic stellate cells.

结果与分析

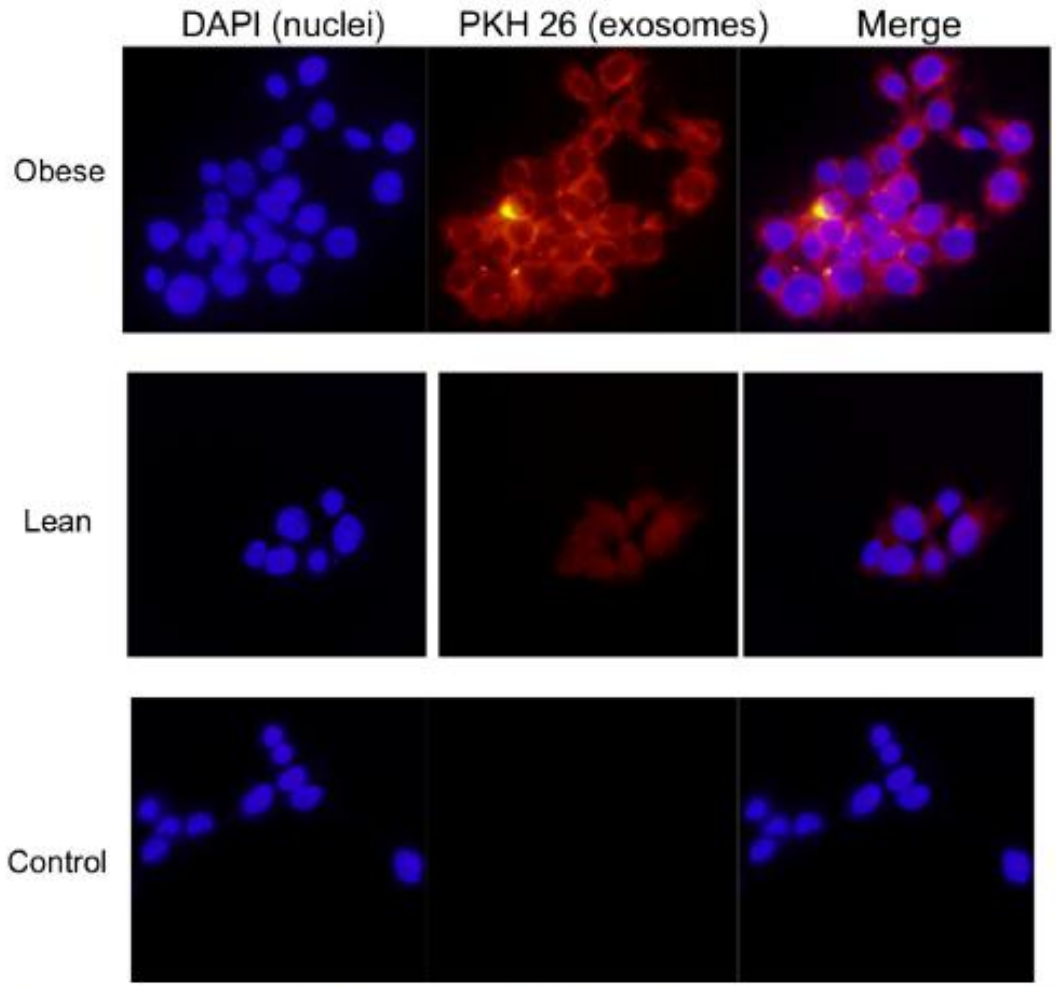

Fig. 1 – Immunofluorescence microscopy images of HepG2 cells after exposure to fluorescent-labeled exosomes.

结果与分析

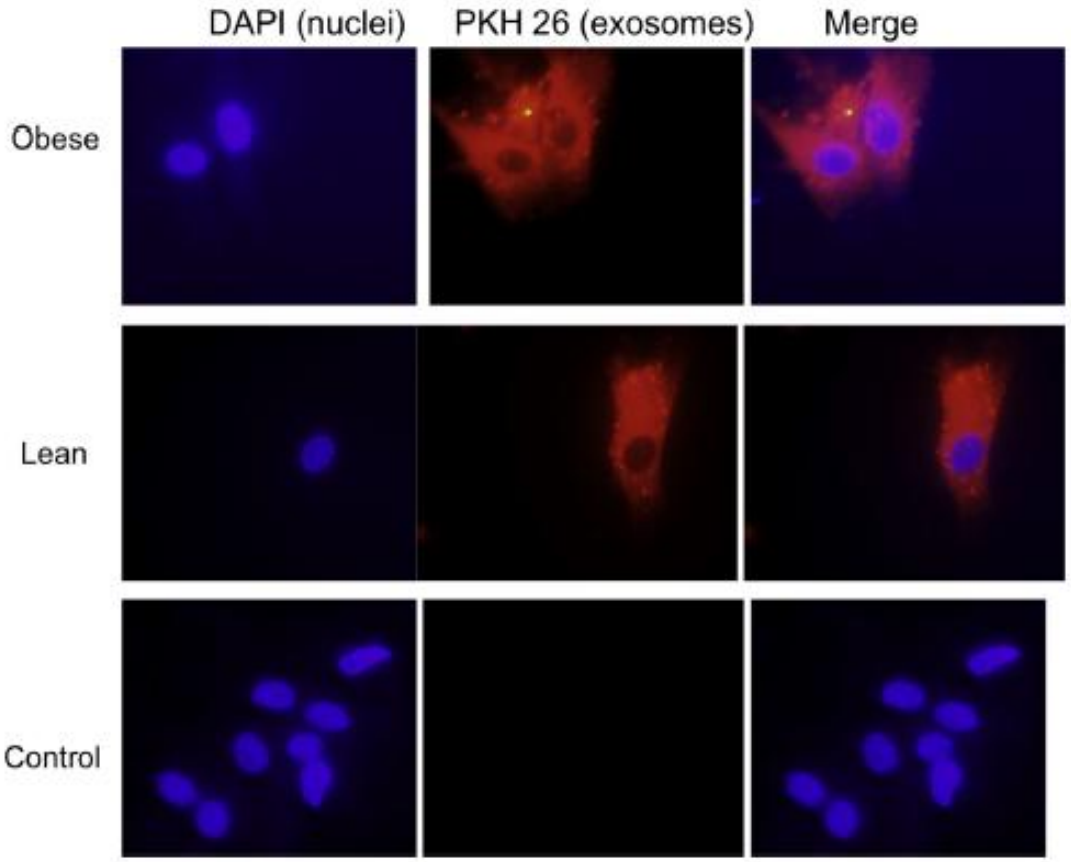

Fig. 2 – Immunofluorescence microscopy images of HHSteC cells after exposure to fluorescent-labeled exosomes.

结果与分析

Table 1 – Changes in expression of TGF-β pathway mediators in HepG2 cells exposed to visceral adipocyte exosomes (Data represent mean fold change ± standard deviation).

Mediator	0.1% dilution		1% dilution		Both doses	
	Fold change	P	Fold change	P	Fold change	P
TIMP-1						
Obese 1	2.82 ± 1.91	0.24	2.64 ± 1.14	**0.04**	2.73 ± 1.41	**0.02**
Obese 2	1.74 ± 0.83	0.31	2.01 ± 0.91	0.16	1.94 ± 0.76	0.08
Obese 3	3.13 ± 1.21	0.08	4.78 ± 0.66	**0.004**	4.36 ± 0.99	**0.002**
Obese 4	4.69 ± 0.003	**0.01**	3.36 ± 0.27	**0.01**	4.02 ± 0.78	**0.004**
All obese	3.24 ± 1.54	**0.008**	3.18 ± 1.34	**0.003**	3.21 ± 1.38	0.026
Lean 1	7.51 ± 1.05	**0.002**	0.93 ± 1.48	0.29	5.32 ± 3.87	0.19
MMP-7						
Obese 1	0.44 ± 0.07	0.46	0.41 ± 0.20	0.41	0.42 ± 0.14	**0.0008**
Obese 2	0.84 ± 0.003	0.6	0.51 ± 0.39	0.69	0.51 ± 0.39	0.40
Obese 3	0.56 ± 0.34	0.62	1.07 ± 0.23	0.85	0.95 ± 0.16	0.62
Obese 4	0.61 ± 0.28	0.51	0.97 ± 0.31	0.74	0.85 ± 0.31	0.41
All obese	0.50 ± 0.10	0.31	0.74 ± 0.38	0.70	0.66 ± 0.33	**0.03**
Lean 1	0.96 ± 0.23	0.55	1.17 ± 0.78	0.94	1.07 ± 0.23	0.80
PAI-1						
Obese 1	0.50 ± 0.10	0.06	1.08 ± 0.26	0.80	0.79 ± 0.36	0.24
Obese 2			0.32 ± 0.06	**0.03**	0.32 ± 0.06	**0.03**
Obese 3	0.50 ± 0.18	0.17	0.67 ± 0.13	0.15	0.60 ± 0.16	0.08
Obese 4	0.82 ± 0.14	0.38	0.76 ± 0.22	0.29	0.79 ± 0.17	0.30
All obese	0.62 ± 0.20	0.09	0.74 ± 0.32	0.18	0.70 ± 0.27	**0.003**
Lean 1	1.00 ± 0.05	0.99	1.11 ± 0.19	0.66	1.06 ± 0.13	0.80
Integrin αvβ-5						
Obese 1	1.60 ± 0.24	0.14	1.79 ± 0.21	0.12	1.71 ± 0.22	0.14
Obese 2			0.94 ± 0.48	0.69	0.94 ± 0.48	0.69
Obese 3	1.31 ± 0.42	0.19	0.95 ± 0.38	0.74	1.04 ± 0.35	0.96
Obese 4	2.00 ± 0.11	0.13	1.34 ± 0.45	0.43	1.68 ± 0.48	0.11
All obese	1.75 ± 0.32	0.13	1.26 ± 0.49	0.53	1.44 ± 0.49	**0.027**
Lean 1	1.17 ± 0.29	0.56			1.17 ± 0.29	0.56

Bold values indicate statistical significance.

结果与分析

Table 2 – Changes in expression of TGF-β pathway mediators in HHSteC cells exposed to visceral adipocyte exosomes (Data represent mean fold change ± standard deviation).

Subject	0.1% dilution		1% dilution	
	Fold change	P	Fold change	P
TIMP-1	2.07 ± 0.72	0.0007	1.51 ± 0.57	0.09
TIMP-4	1.43 ± 0.47	0.02	1.42 ± 0.33	0.0009
Smad-3	1.27 ± 0.22	0.02	1.19 ± 0.23	0.06
Integrin αvβ-5	1.69 ± 0.46	0.0005	1.29 ± 0.26	0.01
Integrin αvβ-8	2.06 ± 0.90	0.013	1.59 ± 0.67	0.02
MMP-9	2.13 ± 0.39	0.01	1.32 ± 0.62	0.38

外泌体与脂肪及肝脏组织互作

这些实验的结果提供新的见解，内脏脂肪细胞的外泌体在NAFLD的发病机制和其他与肥胖有关的疾病中发挥潜在的作用。

外泌体与脂肪合成

Biochemical and Biophysical Research Communications 445 (2014) 327–333 生物化学和生物物理研究通讯

Contents lists available at ScienceDirect

Biochemical and Biophysical Research Communications

journal homepage: www.elsevier.com/locate/ybbrc

Lipid synthesis is promoted by hypoxic adipocyte-derived exosomes in 3T3-L1 cells

Soichi Sano [a], Yasukatsu Izumi [a,b,*], Takehiro Yamaguchi [a], Takanori Yamazaki [a], Masako Tanaka [b], Masayuki Shiota [b], Mayuko Osada-Oka [c], Yasuhiro Nakamura [d], Min Wei [e], Hideki Wanibuchi [e], Hiroshi Iwao [b], Minoru Yoshiyama [a]

[a] Department of Cardiovascular Medicine, Osaka City University Graduate School of Medicine, Osaka, Japan
[b] Department of Pharmacology, Osaka City University Graduate School of Medicine, Osaka, Japan
[c] Food Hygiene and Environmental Health, Kyoto Prefectural University, Graduate School of Life and Environmental Sciences, Kyoto, Japan
[d] Department of Cardiology, Izumi Municipal Hospital, Izumi-Osaka, Japan
[e] Department of Pathology, Osaka City University Graduate School of Medicine, Osaka, Japan

河南师范大学

在3T3-L1细胞中缺氧脂肪细胞来源的外泌体能够促进脂质合成

外泌体与脂肪合成

A B S T R A C T

Hypoxia occurs within adipose tissues as a result of adipocyte hypertrophy and is associated with adipocyte dysfunction in obesity. Here, we examined whether hypoxia affects the characteristics of adipocyte-derived exosomes. Exosomes are nanovesicles secreted from most cell types as an information carrier between donor and recipient cells, containing a variety of proteins as well as genetic materials. Cultured differentiated 3T3-L1 adipocytes were exposed to hypoxic conditions and the protein content of the exosomes produced from these cells was compared by quantitative proteomic analysis. A total of 231 proteins were identified in the adipocyte-derived exosomes. Some of these proteins showed altered expression levels under hypoxic conditions. These results were confirmed by immunoblot analysis. Especially, hypoxic adipocyte-released exosomes were enriched in enzymes related to *de novo* lipogenesis such as acetyl-CoA carboxylase, glucose-6-phosphate dehydrogenase, and fatty acid synthase (FASN). The total amount of proteins secreted from exosomes increased by 3–4-fold under hypoxic conditions. Moreover, hypoxia-derived exosomes promoted lipid accumulation in recipient 3T3-L1 adipocytes, compared with those produced under normoxic conditions. FASN levels were increased in undifferentiated 3T3-L1 cells treated with FASN-containing hypoxic adipocytes-derived exosomes. This is a study to characterize the proteomic profiles of adipocyte-derived exosomes. Exosomal proteins derived from hypoxic adipocytes may affect lipogenic activity in neighboring preadipocytes and adipocytes.

外泌体与脂肪代谢

结 果

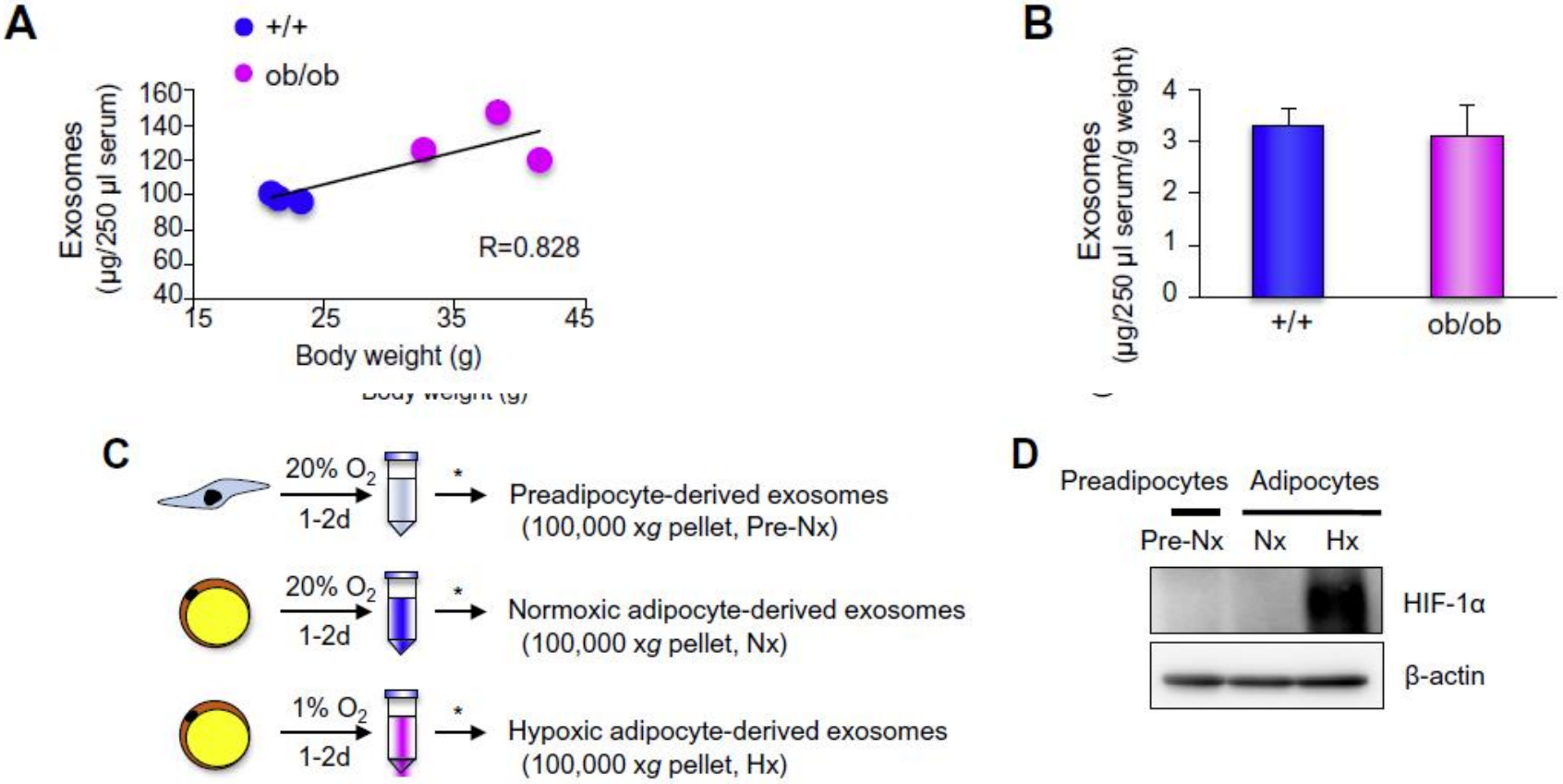

Fig. 1. Characterization of adipocyte-derived exosomes under hypoxic conditions. (A) Serum exosomes were purified from 7-week-old WT (+/+) and ob/ob mice using ExoQuick™ reagent and exosomal proteins per unit serum were determined. The graph represents the ratio of protein in serum exosomes for each group. Values are mean ± SD (each $n = 3$). $^*P < 0.01$. (B) Data in (A) are corrected by body weight. Values are mean ± SD. (C) Flow chart of differential centrifugation-based protocol for exosome purification from culture supernatants. (D) Expression level of HIF-1α protein in 3T3-L1 preadipocytes and adipocytes cultured under normoxic or hypoxic conditions for 24 h. (E) Morphology of 3T3-L1 preadipocyte- and adipocyte-derived exosomes from normoxic or hypoxic conditions visualized by electron microscopy. Scale bar, 100 nm. (F) Protein concentrations in preadipocyte- and adipocyte-derived exosomes generated under normoxic or hypoxic conditions. The graph represents the ratio of normoxic exosomal proteins to hypoxic proteins. Values are mean ± SD ($n = 3$). $^*P < 0.01$. 3T3-L1 adipocytes 10 days post differentiation were used for assays in (C)–(F).

结 果

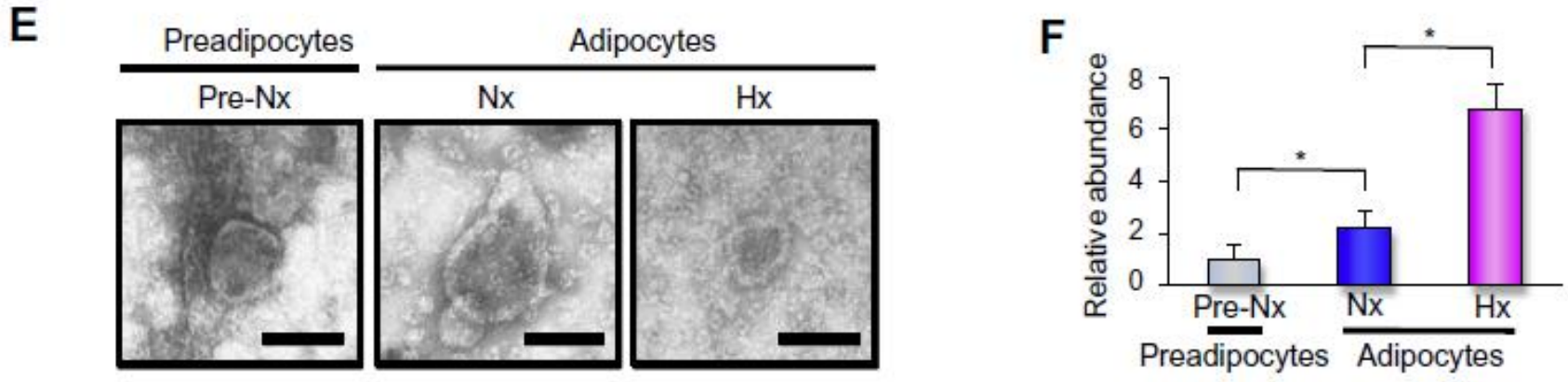

Fig. 1. Characterization of adipocyte-derived exosomes under hypoxic conditions. (A) Serum exosomes were purified from 7-week-old WT (+/+) and ob/ob mice using ExoQuick™ reagent and exosomal proteins per unit serum were determined. The graph represents the ratio of protein in serum exosomes for each group. Values are mean ± SD (each $n = 3$). $^*P < 0.01$. (B) Data in (A) are corrected by body weight. Values are mean ± SD. (C) Flow chart of differential centrifugation-based protocol for exosome purification from culture supernatants. (D) Expression level of HIF-1α protein in 3T3-L1 preadipocytes and adipocytes cultured under normoxic or hypoxic conditions for 24 h. (E) Morphology of 3T3-L1 preadipocyte- and adipocyte-derived exosomes from normoxic or hypoxic conditions visualized by electron microscopy. Scale bar, 100 nm. (F) Protein concentrations in preadipocyte- and adipocyte-derived exosomes generated under normoxic or hypoxic conditions. The graph represents the ratio of normoxic exosomal proteins to hypoxic proteins. Values are mean ± SD ($n = 3$). $^*P < 0.01$. 3T3-L1 adipocytes 10 days post differentiation were used for assays in (C)–(F).

在低氧条件下的3T3-L1脂肪细胞来源的外泌体蛋白水平增加3-4倍

结 果

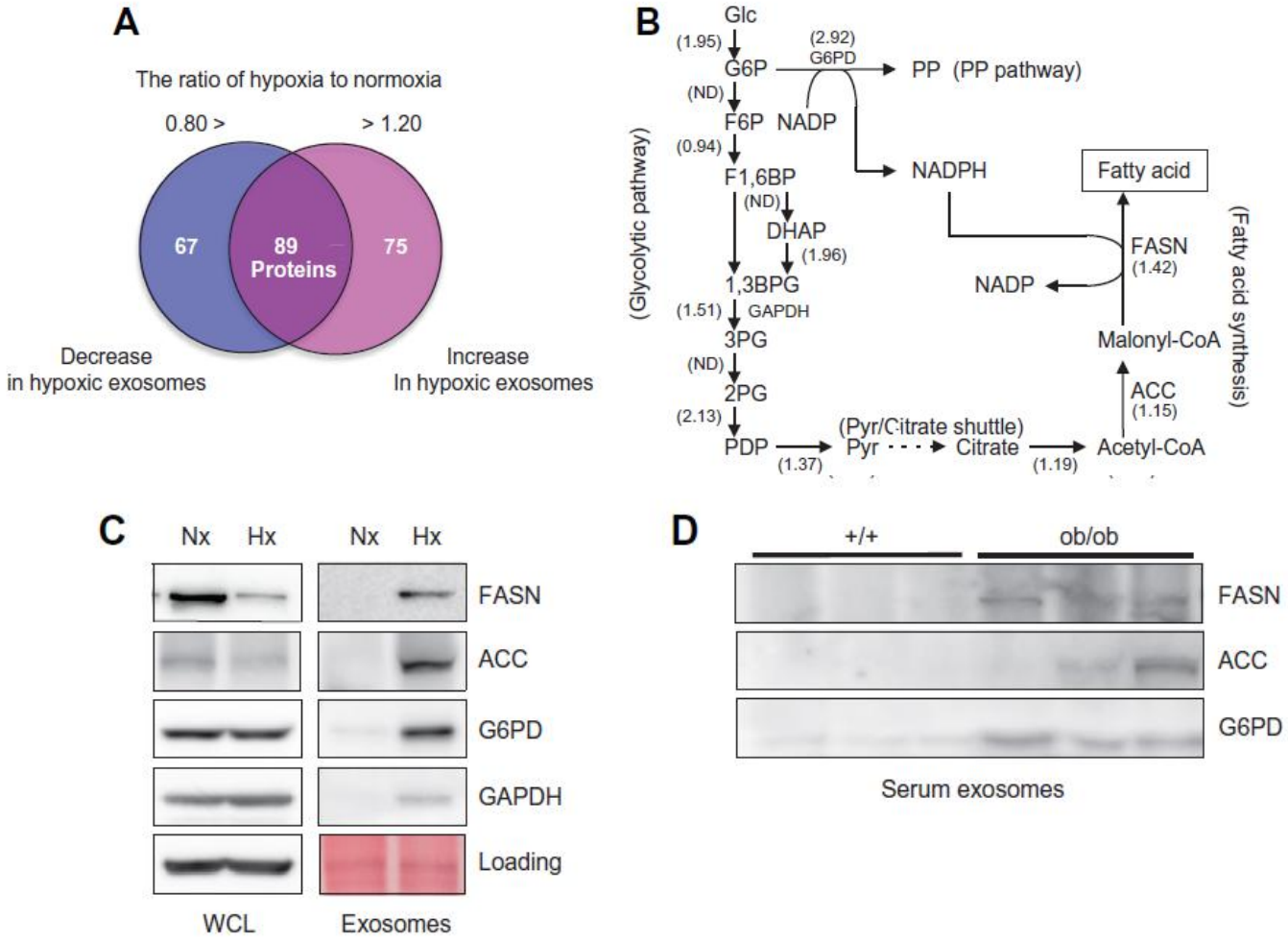

Fig. 2. Proteomic analysis of adipocyte-derived exosomes from normoxic or hypoxic conditions. (A) Comparison of proteins identified in adipocyte-derived exosomes under normoxic or hypoxic conditions. A total of 231 proteins were identified; a ratio under 0.80 was considered a decrease, while that over 1.20 was considered an increase. (B) Metabolic pathways leading to fatty acid production and its related enzymes. (C) FASN, ACC, and G6PD expression levels in whole cell lysates (WCL) and exosomes by Western blot analysis. ImmunoGold is a control blot of exosomal proteins. (D) FASN, G6PD, and GAPDH expression levels in serum exosomes from 7-week-old WT (+/+) and ob/ob mice by Western blot analysis.

结 果

Table 1
Up-regulated proteins in hypoxic adipocyte-derived exosomes, compared to control (>1.20-fold).

Accession numbers	Protein names	Unique peptdes detected	Sequencecoverage%	116:114 (Nx:Hx)	Expectation-value
gi|93102409	Fatty acid synthase	18	19	1.42	1.70E-22
gi|31981562	Pyruvate kinase isozymes M1/M2 isoform 1	6	22	1.37	1.32E-05
gi|33859482	Elongation factor 2	5	8	1.53	1.34E-05
gi|70794816	Uncharacterized protein LOC433182	5	21	1.34	3.62E-05
gi|6679937	Glyceraldehyde-3-phosphate dehydrogenase	4	21	1.51	1.91E-05
gi|6678483	Ubiquitin-like modifier-activating enzyme 1 isoform 1	4	10	1.51	2.67E-06
gi|6755901	Tubulin alpha-1A chain	4	18	1.41	5.03E-05
gi|309264022	PREDICTED: 40S ribosomal protein SA-like	3	19	1.88	2.15E-04
gi|31980648	ATP synthase subunit beta, mitochondrial precursor	3	10	1.81	1.04E-03
gi|52353955	D-3-phosphoglycerate dehydrogenase	3	8	1.68	8.92E-03

This table included up-regulated proteins having at least 3 unique peptides with ⩾99% confidence using ProteinPilot 2.0 software. Accession numbers are from the NCBI database. For additional information, see Supplementary Tables 1A and 2).

结 果

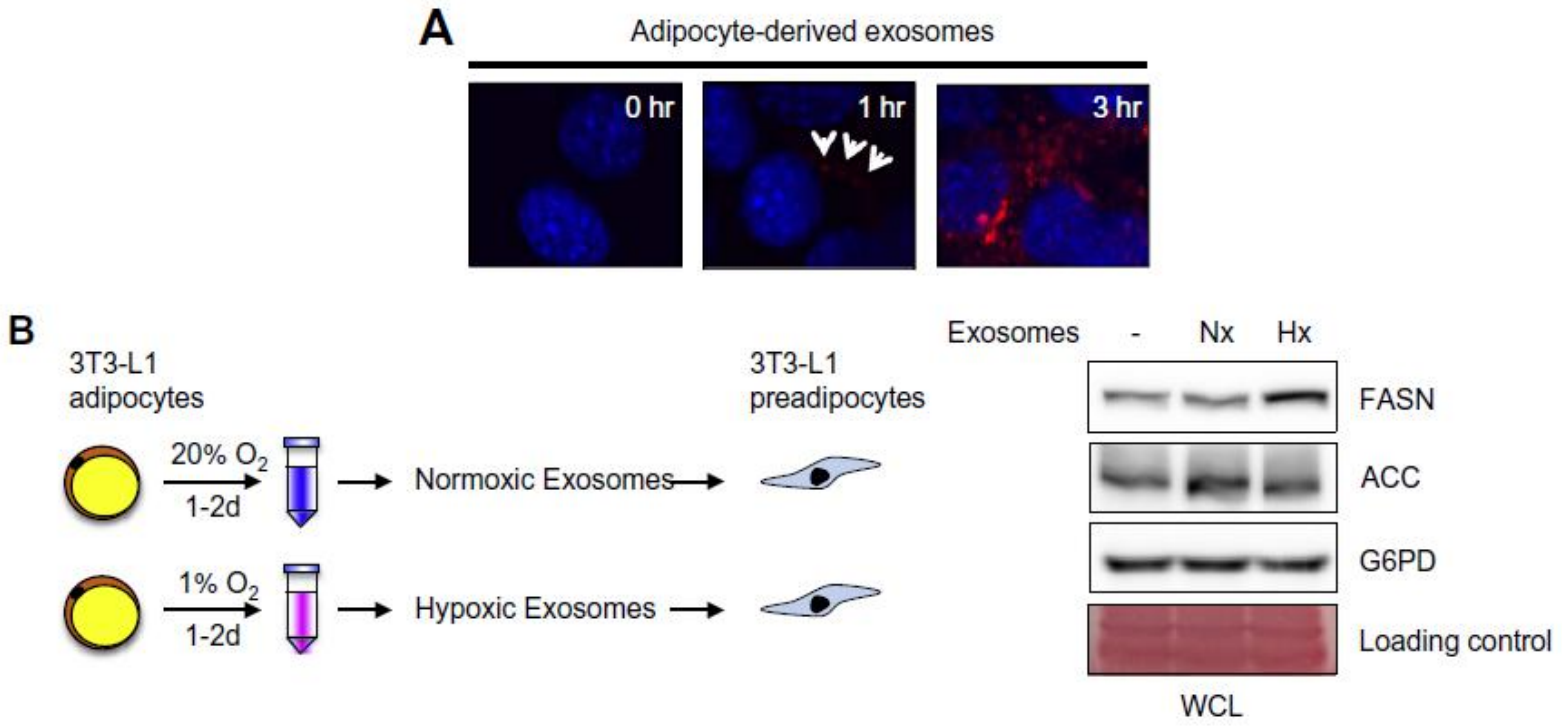
A
Adipocyte-derived exosomes
0 hr
1 hr
3 hr
B
3T3-L1
adipocytes
20% O2
1-2d
Normoxic Exosomes
3T3-L1
preadipocytes
1% O2
1-2d
Hypoxic Exosomes
Exosomes - Nx Hx
FASN
ACC
G6PD
Loading control
WCL

结 果

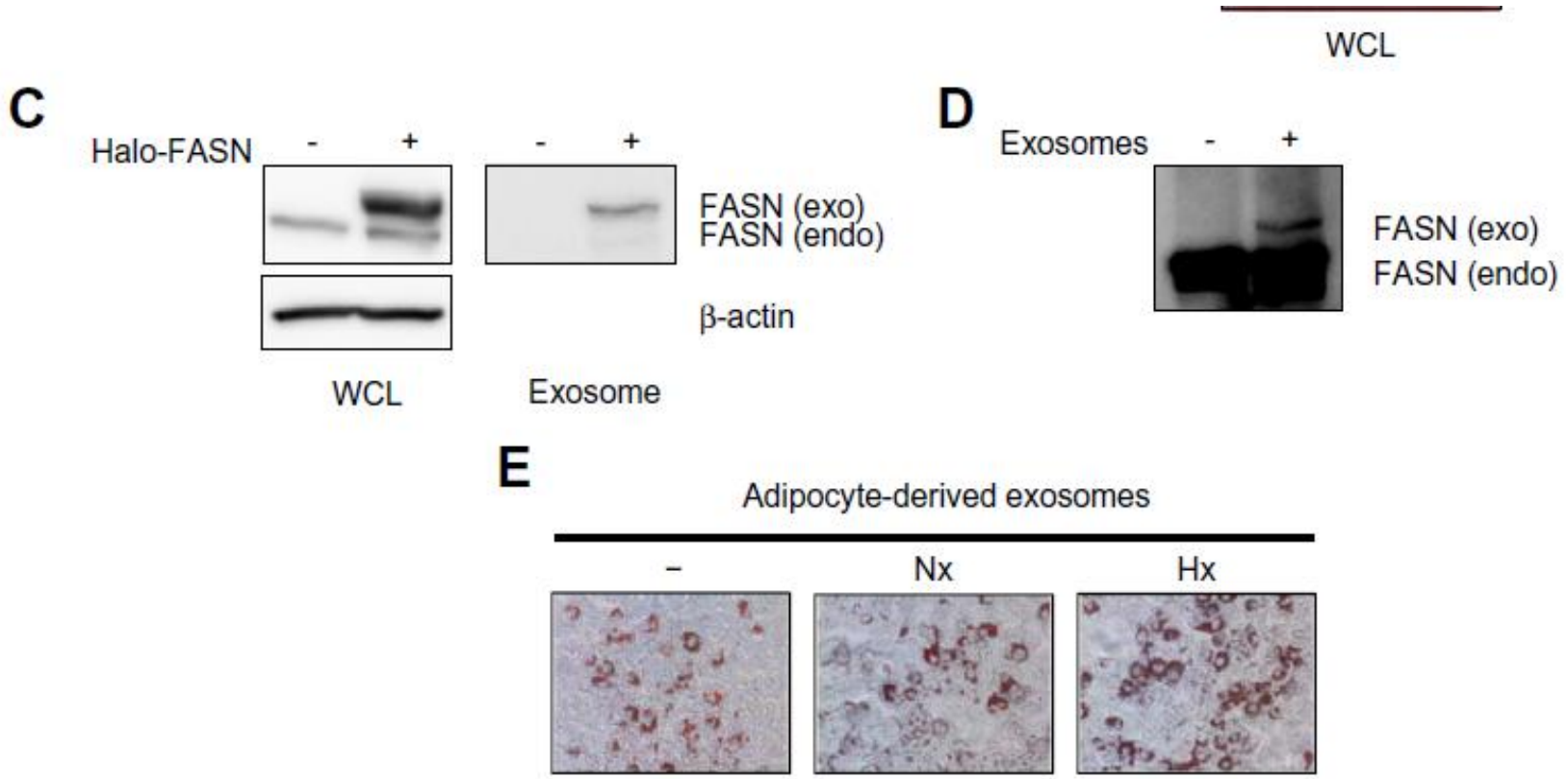

Fig. 3. Increased iipid accumulation in adipocytes treated with hypoxic adipocyte-derived exosomes. (A) Time-dependent uptake of adipocyte-derived exosomes in 3T3-L1 preadipocytes. PKH26-labeled exosomes (*red*) were added to 3T3-L1 cells and incubated as indicated. Cells were fixed and stained for nuclei (DAPI, *blue*). (B) Lysates from 3T3-L1 preadipocytes after incubation with exosomes from differentiated 3T3-L1 adipocytes cultured under normoxic or hypoxic conditions for 48 h were subjected to Western blot analysis using the indicated antibodies (FASN, ACC, and G6PD). (C) HEK 293T cells were transfected with plasmid encoding Halo-FASN. In Western blotting analysis, the same amounts of cell lysates (20 μg) and exosomes (1 μg) were loaded into the indicated lanes. (D) Lysates from 3T3-L1 preadipocytes after incubation with exosomes from HEK 293T cells transfected with plasmid encoding Halo-FASN were subjected to Western blot analysis using the anti-FASN antibody. (E) 3T3-L1 cells were induced to differentiate after confluence with a cocktail of hormones/steroids as described in the Section 2 for 6 days. 100 μg of adipocyte-derived exosomes from normoxic or hypoxic conditions was added to culture medium every 2 days. Original magnificaiton 100×.

讨 论

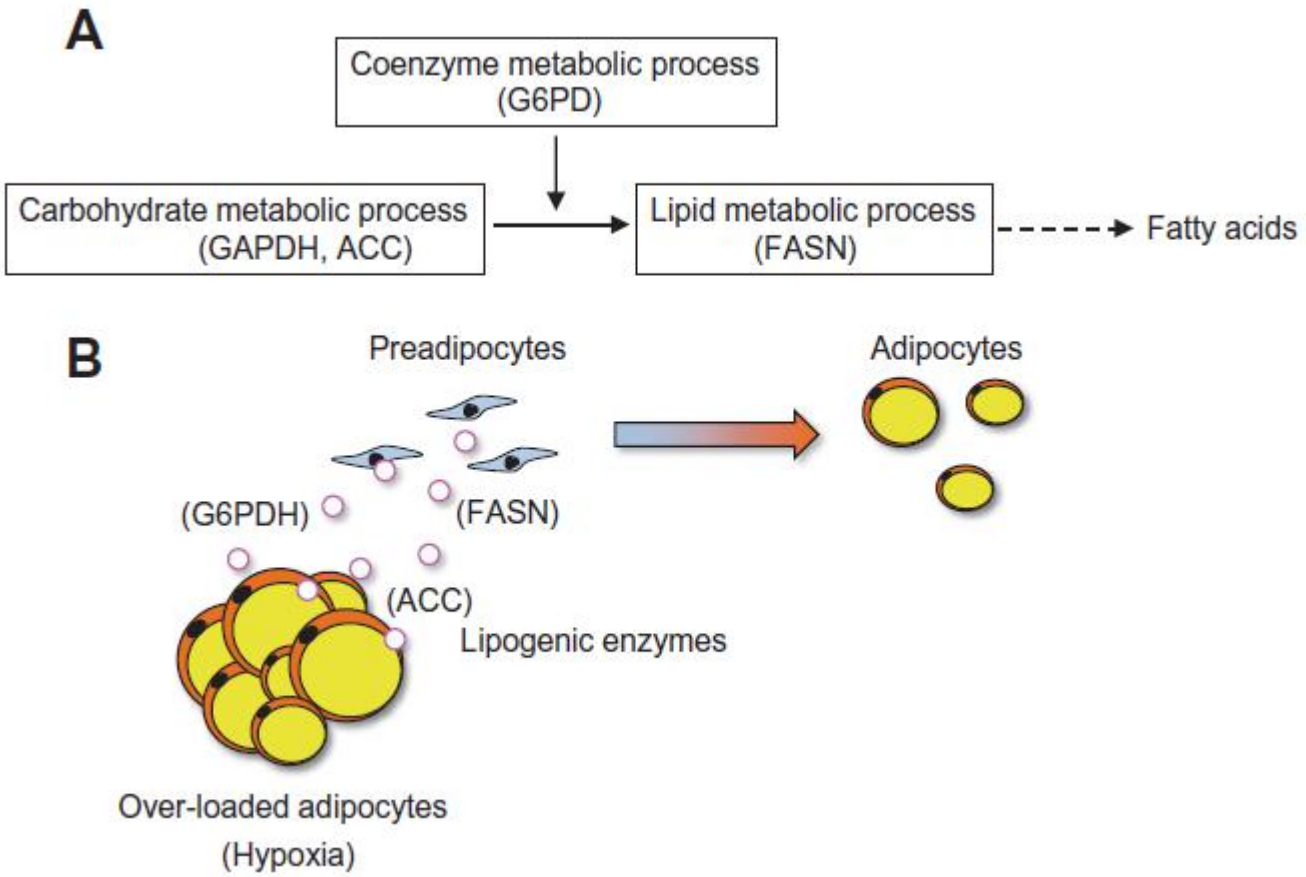

Fig. 4. Schematic representation of this study. (A) Relationship between ACC, G6PD, and FASN and *de novo* lipogenesis. (B) Promotion of lipid accumulation in preadipocytes or small adipocytes due to hypoxic adipocyte-derived exosomes.

Thank You !